Description of Si-O Bond Breakage Using Pair-Wise Interatomic Potentials Under Consideration of the Whole Crystal

S.E. Tyaginov, W. Gös, T. Grasser
Christian Doppler Laboratory for TCAD at the Institute for Microelectronics
TU Wien
Vienna, Austria
phone: (43)-(1)-58801-36025, e-mail: tyaginov@iue.tuwien.ac.at

V. Sverdlov, Ph. Schwaha, R. Heinzl, F. Stimpfl
Institute for Microelectronics
TU Wien
Vienna, Austria

***Abstract*—We extend the McPherson model in a manner to capture the effect of the whole surrounding lattice on the silicon-oxygen bond-breakage energetics. It is shown that the Mie-Grüneisen potential with the constants used in the original version of the model is not suitable under the consideration of the whole crystal. Other empirical pair-wise interatomic potentials, namely TTAM and BKS have been tested for the analysis of the bond rupture energetics. It is shown that the secondary minimum corresponding to the transition of the Si atom from the 4-fold to the 3-fold coordinated position occurs in a different direction with a rather high activation energy (~ 6 eV). The tunneling of the Si ion between the primary and the secondary minima has been treated within the WKB approximation. We demonstrate that the contribution of neighboring SiO_4 tetrahedrons substantially decreases the breakage rate, making bond rupture by means of an electric field alone practically impossible. Therefore, the common action of an electric field and another contribution (bond weakening by hole capture, structural disorder and energy deposited by particles) is essential for Si-O bond-breakage.**

Keywords-Si-O bond, bond-breakage, WKB, pair-wise potentials, TTAM, BKS, Mie-Grüneisen potential, silicon dioxide, tunneling

I. INTRODUCTION

So far there is no comprehensive SiO_2 degradation model reconciling contradictions related to the main competing approaches: anode hole injection [1,2] and hydrogen release [3] models assuming that energy delivered by particles (hot carriers and/or hydrogen) is responsible for oxide damage vs. the thermo-chemical model [4,5] assuming that the electric field is the sole driving force. Since in the literature there is a bulk of diverse experimental data supporting each of these concepts one may conclude that all these components are essentially presented as various contributors to breakdown.

At the same time, the breakage of the silicon-oxygen bond is one of the most crucial issues in the field of reliability of SiO_2 films. Several research groups claim that Si-O bond rupture is the essential contributor to hot-carrier-induced (HCI) damage [2,6-8] as well as to time-dependent-dielectric-breakdown (TDDB) [4,5,8-10]. A recently proposed model for Si-O bond-breakage by McPherson [4,5] considers binding potentials as a function of the Si ion displacement from its equilibrium position (EP) in the center of SiO_4 tetrahedron. For the description of the interaction between the silicon and the 4 surrounding oxygen ions the Mie-Grüneisen pair-wise interatomic potential has been employed [4]. Thus the potential energy for the interaction between Si and O ions separated by the distance r is:

$$\Phi(r) = \Phi_B\left[A\left(\frac{r_0}{r}\right)^9 - B\left(\frac{r_0}{r}\right)^2 - C\left(\frac{r_0}{r}\right)\right], \qquad (1)$$

where Φ_B = 5.4 eV and r_0 = 1.7 Å are the strength and the length of the Si-O bond and the constants $\{A,B,C\}$ are determined by the following three conditions:

1. The potential energy for the Si-O interaction at the Si EP corresponds to the bond strength, i.e. $\Phi(r_0) = \Phi_B$.
2. Constants $\{A,B,C\}$ should warrant a zero force on the silicon atom in equilibrium: $\partial\Phi/\partial r\big|_{r=r_0} = 0$
3. Finally, the bond polarity $f_o^* = C/(B + C)$ at $r = r_0$ is equal to its conventional value of 0.6.

Solving the system of 3 equations with 3 unknowns one finds the parameters $\{A,B,C\}$:

$$A = \frac{2 - f_0^*}{9 - (2 - f_0^*)}, B = 9\frac{1 - f_0^*}{9 - (2 - f_0^*)}, C = 9\frac{f_0^*}{1 - (2 - f_0^*)} \quad (2)$$

For our further purposes it is convenient to rewrite the Mie-Grüneisen potential in the following form:

$$\Phi_{\text{SiO}}(r) = Q_{Si}^{(9)}Q_O^{(9)}/r^9 - Q_{Si}^{(2)}Q_O^{(2)}/r^2 - Q_{Si}^{(1)}Q_O^{(1)}/r, \quad (3)$$

where $Q_{Si}^{(m)}/Q_O^{(m)}$ are "effective charges" of Si/O ions for the terms of power m related to the constants used in the original form through these equations:

$$Q_{Si}^{(9)}Q_O^{(9)} = \Phi_B r_0^9 A \quad (4a)$$
$$Q_{Si}^{(2)}Q_O^{(2)} = \Phi_B r_0^2 B \quad (4b)$$
$$Q_{Si}^{(1)}Q_O^{(1)} = \Phi_B r_0^1 C \quad (4c)$$

Note that since the McPherson Model does not consider Si-Si and O-O interactions, "effective charges" themselves do not enter the model and the products of them have been used as quantities characterizing the Si-O bond as a whole. While deriving an extended version of the model we take into account the products of parameters, such as $Q_{Si}^{(m)}Q_O^{(m)}$, since exactly these products are involved into expressions for Si-Si and O-O potentials.

In the original version of the McPherson model the symmetry of a single tetrahedron determines the potential profile acting on the Si ion. One may "mark" one of the O ions and distinguish the contributions in the potential from this ion and 3 other ions situated at the opposite face. If we now move the Si ion away from its equilibrium position perpendicular to this O_3 plane (Fig. 1) the contributions of these in-plane ions are identical due to the symmetry of the equilateral triangle with respect to the direction of the ion shift. Thus, this portion of the energy displays two minima corresponding to the saddle positions of the Si ion in front (the equilibrium position) and beyond the plane separated by a maximum (Si penetrates the O_3 plane). The contribution of the "marked" oxygen ion deepens the primary minimum and simultaneously makes the second one shallower. The total potential energy of the interaction of the Si ion with four surrounding O ions is depicted in Fig. 2 and reveals two minima separated by a barrier of ~ 2.3 eV.

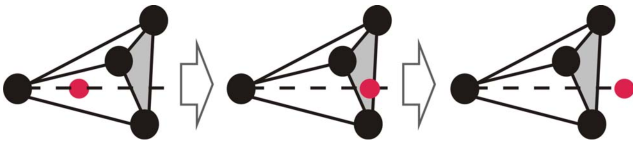

Fig. 1. Transition of the Si ion from its 4-fold equilibrium position perpendicular and beyond the O_3 plane to the 3-fold coordination.

Within the McPherson model the transition of the Si ion from the 4-fold coordinated position in the center of the SiO_4

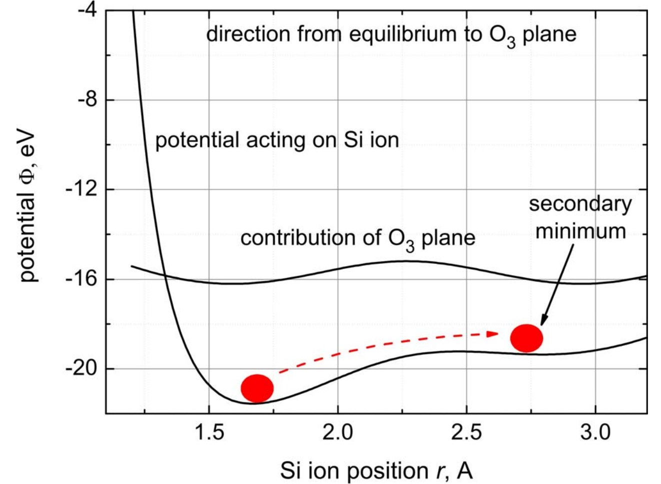

Fig. 2. Potential acting on the Si ion from 4 neighboring O ions as a function of its displacement in the direction from the center of the SiO_4 tetrahedron perpendicular to the O_3 plane. The contribution of the 3 O ions in this plane is also depicted.

tetrahedron to the 3-fold coordination beyond the plane is interpreted as the rupture of the Si-O bond followed by formation of a Si-Si bridge [4,5,8-10]. The bond-breakage has been treated as a superposition of thermionic emission and tunneling of the Si ion between the primary and the secondary minima. For the calculation of the breakage rate the quasi-classical WKB approach was employed.

In spite of the intuitive appeal of the model which is able to reproduce the reduction of the activation energy with the electric field and hence the linear dependence of the logarithmic time-to-breakdown vs. field [9,10] it is obvious that the contribution of the whole lattice substantially changes the energetics of Si-O bond. In fact, the neighboring Si ions are situated at a distance of only 3.2 Å from the center of the SiO_4 tetrahedron and – assuming that the charge of Si ion is twice larger than the one of an O ion – their contribution to the potential energy considerably shifts it upwards. Moreover, as the Si ion moves towards and beyond the plane the contribution of one of these Si ions substantially increases and thus changes the energetical position of the secondary minimum. Since in the McPherson model the direction in which the saddle point occurs is defined by the symmetry of a single tetrahedron, under the consideration of the whole crystal the secondary minimum is expected to occur in a different direction.

Note also that taking into account just one SiO_4 tetrahedron excludes the possibility to construct the potential profile acting on an oxygen ion. Such a profile is useful while testing whether the constants in the Mie-Grüneisen potential found under the consideration of the whole lattice are adequate, i.e. warrant a stable atomic configuration (discussed below). Moreover, although in this paper we restricted ourselves by consideration of a formation of a Si-Si bridge, the possibility of a generation of oxygen-excess configurations, i.e. Si-O-O-Si complexes also exists. Such an oxygen-excess

is to be related to a transition of O ion between the primary and the secondary minima featured by the potential profile.

To summarize, the main scope of this paper is to extend the original McPherson model in a way to capture the effect of the whole lattice on Si-O energetics. This approach will be referred to as the Extended McPherson Model throughout this work.

II. General Considerations

While taking into account the whole surrounding network one should extend the initial Mie-Grüneisen potential in order to capture also Si-Si and O-O interactions (maintaining the form of (3):

$$\Phi_{SiSi}(r) = Q_{Si}^{(9)}Q_{Si}^{(9)}/r^9 - Q_{Si}^{(2)}Q_{Si}^{(2)}/r^2 - Q_{Si}^{(1)}Q_{Si}^{(1)}/r \quad (5)$$

$$\Phi_{OO}(r) = Q_{O}^{(9)}Q_{O}^{(9)}/r^9 - Q_{O}^{(2)}Q_{O}^{(2)}/r^2 - Q_{O}^{(1)}Q_{oi}^{(1)}/r \quad (6)$$

Combining (3)-(5) we now have a set of pair-wise interatomic potentials for description of the interactions in SiO_2. In general there are 6 independent constants: there are 2 types of ions and each of them is characterize by the 3 “effective charges”.

Another requirement is the condition of convergence of the electrostatic energy, i.e. for each term of the *m*-th order corresponding sums must necessary converge [11,12]:

$$U^{(m)} = \frac{1}{2}\sum_{n_1,n_2,n_3}\sum_i\sum_j^{i\neq j}\frac{Q_i^{(m)}Q_j^{(m)}}{|\vec{r}_i - \vec{r}_j + \vec{n}|^m}, \quad (7)$$

Here $\boldsymbol{n} = n_1\boldsymbol{t}_1 + n_2\boldsymbol{t}_2 + n_3\boldsymbol{t}_3$ spans all primitive cells of the crystal, n_1, n_2, n_3 denote arbitrary integers, $\boldsymbol{t}_1$, $\boldsymbol{t}_2$, and $\boldsymbol{t}_3$ are the primitive translation vectors. Indices i, j list the ions in one primitive cell, i.e. run from 1 to 9 since each SiO_2 unit cell includes 9 ions. Note that in the sums of (7) self-interacting terms must be excluded, in other words, components with $i = j$ for $\boldsymbol{n} = \boldsymbol{0}$ are omitted [11-12].

Because of electro-neutrality of a primitive cell of α-SiO_2 containing 3 Si and 6 O ions one may conclude $Q_{Si}^{(m)} = -2Q_O^{(m)}$ and thus the number of independent constants in the Mie-Grüneisen potential is reduced to 3 and – similar to the original McPherson model – one needs 3 conditions to find these constants. Since (3,5,6) operate with products $Q_i^{(m)}Q_j^{(m)}$ we will find $Q_{Si}^{(m)}Q_O^{(m)}$ (the Mie-Grüneisen potential written in the from (1) operates with constants $\{A,B,C\}$ which are equal to $Q_{Si}^{(m)}Q_O^{(m)}/(\Phi_B \cdot r_0^m)$) and express other products as $Q_O^{(m)}Q_O^{(m)} = -1/2Q_{Si}^{(m)}Q_O^{(m)}$ and $Q_{Si}^{(m)}Q_{Si}^{(m)} = -2Q_{Si}^{(m)}Q_O^{(m)}$.

Note here, that the conditions used by McPherson for the determination of the constants are not suitable under consideration of the whole lattice. In fact, introduction of the bond strength Φ_B is correct only in the case of a single bond and, when taking into account the whole crystal, i.e. contributions of other neighbors to the energetics of a bond, one should introduce another quantity which is a property of the whole crystal such as e.g. the cohesion energy. The requirement of zero-force acting on the Si ions in EPs will be automatically satisfied due to the crystal symmetry and thus does not provide any additional information. Moreover, from a formal mathematical point of view this extremum could correspond to a maximum of energy (instead of its minimum) if a wrong set of constants in the Mie-Grüneisen potential is used as will be shown below. To summarize, for the determination of the constants $\{A_1,A_2,A_3\}$ (or parameters $Q_{Si}^{(m)}Q_O^{(m)}$) one should use other conditions for the calibration of the Mie-Grüneisen potential in our extended model.

Another important issue is the calculation of the potential acting on an ion from the rest of the crystal. Let us consider an ion of type j with the corresponding position $\boldsymbol{r}$ which we assume to be in the cell with $\mathbf{n} = \mathbf{0}$. Similar to (7), for the contribution related to the term of the *m*-th order one writes (the term with $i = j$ for $\boldsymbol{n} = \boldsymbol{0}$ is omitted):

$$\Phi_j^{(m)} = \sum_{n_1,n_2,n_3}\sum_i \frac{Q_i^{(m)}Q_j^{(m)}}{|\vec{r}_i - \vec{r} + \vec{n}|^m}. \quad (8)$$

Since the series employed in (7,8) are only conditionally convergent [11] the summation cannot be performed in an arbitrary order. Instead, the summation is to be made in the certain sequence: first one should complete the summation over one unit cell (which is neutral) and only then proceed to another one. In other words, it is necessary to calculate first the internal sum over atoms in a cell (i.e. over i in (8) and then the external one over the whole lattice (over n_1, n_2, n_3). It is worth mentioning that calculations of e.g. (8) in a manner which presumes taking into account only terms within a sphere of a predefined cutoff radius r_{cut} in the real space, i.e. terms with $|\boldsymbol{r}_i - \boldsymbol{r} + \boldsymbol{n}| < \boldsymbol{r}_{cut}$, would lead to large oscillation of the result depending on r_{cu} [11]. For the correct evaluations of energy (7) and potential (8) one may also use the Ewald summation rule (see e.g. [11,12]).

III. Constants employed in McPherson model

As an initial step in the choice of the constants of the extended model we employ the constants used in the original McPherson model [4,5]. The parameters $Q_{Si}^{(m)}Q_O^{(m)}$ based on the values of $\{A,B,C\}$ borrowed from [4] are listed in the Table I. The potentials acting on the Si and O ions from the rest of the crystal as a function of the ion displacement in the direction from the EP of Si perpendicular to the O_3 plane are depicted in Fig. 3a and b, respectively.

Table I. Constants for the Mie-Grüneisen pair-wise potentials borrowed from the original McPherson model {*A*,*B*,*C*} and rewritten in a suitable for the extended model form, i.e. in the form $Q_{Si}^{(m)}Q_{O}^{(m)}$.

Power of term, *m*	McPherson Model, {*A*,*B*,*C*}	Extended McPherson model, $Q_{Si}^{(m)}Q_{O}^{(m)}$
9	0.184 [dimensionless]	117.964 eV·Å^9
2	0.474 [dimensionless]	-7.392 eV·Å^2
1	0.711 [dimensionless]	-6.523 eV·Å

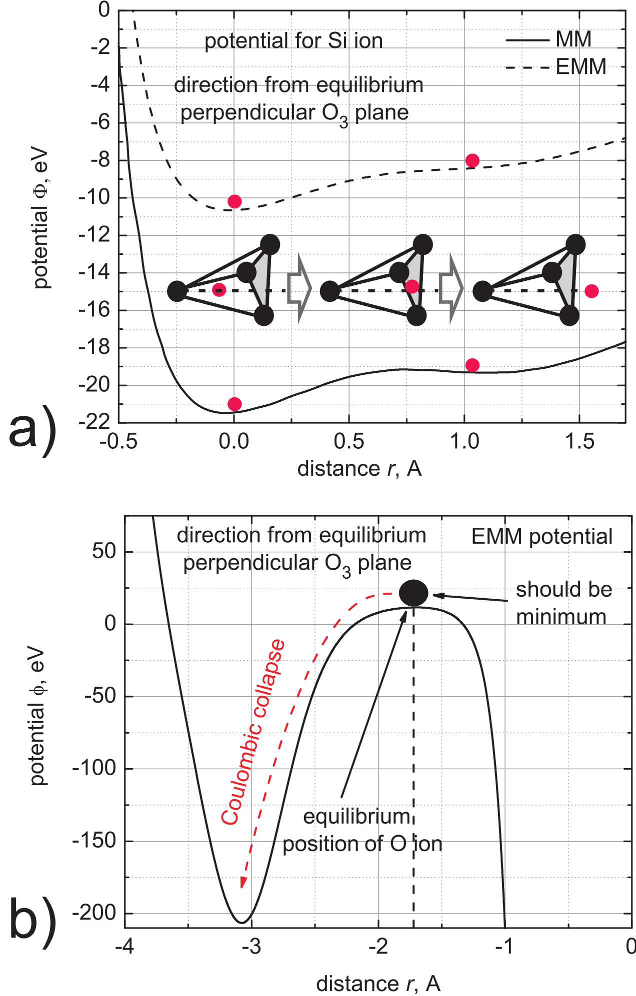

Fig. 3. Potential acting on Si (a) and O (b) ions as a function of their displacement in the direction from the center of SiO_4 tetrahedron perpendicular to the O_3 plane calculated within McPherson model and the extended version with the constants borrowed from the original version of the McPherson model.

The potential profile for a Si ion (Fig. 3a) obtained with the extended McPherson model seems to be reasonable and demonstrates a ledge at the same position as observed in the McPherson model. However, the minimum of potential energy is substantially shifted upwards due to the contribution of the positively charged Si ions. As a consequence, only ~ 10 eV are needed to remove Si ion from the silica network to infinity, a contradiction to the fact that the cohesion energy of α-SiO_2 (energy needed to decompose the crystal into separated atoms) lies in the range of 18.0…19.1 eV/formula unit [13,14].

The potential profile for O (Fig. 3b) reveals the energy maximum at a position corresponding to the ion equilibrium. Hence the O atom drops to the well formed by Si ions (a so-called Coulombic collapse) meaning that this atomic configuration is instable in terms of the extended model with McPherson constants. To avoid Coulombic collapse while constructing an interatomic potential one requires a sufficiently high separating barrier between the equilibrium position of an ion and another minimum formed by attractive components of the interatomic potential (shown in Fig. 3b). Another consequence of the choice of the McPherson constants is a negative value of cohesion energy calculated within the extended model.

These considerations suggest that in the case of the Mie-Grüneisen potential for the whole lattice, one has to find constants by calibration to well-known material properties, e.g. on cohesion energy and/or elastic constants [15]. One may also consider results obtained with density functional theory (DFT) and/or molecular dynamics (MD) (for such purposes a DFT coupled with MD is conventionally used) [16]. However, a more convenient and straightforward way is to use widely-accepted pair-wise potentials, namely potentials proposed by Tsuneyuki, Tsukada, Aoki and Matsui (TTAM) and by van Beest, Kramer and van Santen (BKS) [17,18] constructed just in a manner to reproduce DFT results [17-20].

IV. Usage of TTAM and BKS potentials

Tsuneyuki and co-workers [17] as well as van Beest et al [18] using *ab initio* quantum-chemical calculations developed bulk force field and extracted pair-wise interatomic potentials for large silicon clusters. These potentials have been applied to study properties of diverse polymorphs of silicon dioxide, namely of α-quartz, α-cristobalite, coesite, etc.

For the extension of the McPherson model for the calculations of the potential acting on a certain ion from the rest of the crystal we employed various versions of the TTAM potential and the initial version of BKS. Various forms of TTAM/BKS potentials have the same functional structure including the Coulomb (k converts e^2Å^{-1} into eV; Q_{Si} = +2.4·|e| and Q_{Si} = -1.2·|e| are effective charges of ions and e is the electronic charge), Bukcingham and van der Waals terms [17-20]:

$$\Phi_{i,j}(r_{ij}) = kQ_iQ_j / r_{ij} + \alpha_{ij}e^{-\beta_{ij}r_{ij}} - \gamma_{ij} / r_{ij}^6, \qquad (9)$$

differing only in parameters α_{ij}, β_{ij}, γ_{ij} (see Table II). For instance, BKS (and the Z1 modification of TTAM proposed by Zhu and co-workers [20]) does not consider Si-Si interactions.

Table II. Parameters of various versions of TTAM/BKS potentials used in the calculations of the potential acting on a single ion from the rest of the crystal [17-20].

	α_{ij}	β_{ij}	γ_{ij}
Si-Si TTAM	$8.7235\cdot10^{8}$	15.2207	23.30
Si-Si BKS	0	0	0
Si-Si Z1-TTAM	0	0	0
Si-Si B-TTAM	$7.950\cdot10^{4}$	4.975	446.780
Si-O TTAM	10721.5	4.7959	70.7343
Si-O BKS	18003.8	4.8738	133.538
Si-O Z1-TTAM	7149.0	4.7864	27.661
Si-O FB-TTAM	10450.0	4.8077	63.047
O-O TTAM	1756.90	2.8464	214.736
O-O BKS	1388.773	2.760	175.00
O-O FB-TTAM	1428.0	2.7933	41.374
O-O Z1-TTAM	1359.0	2.8086	215.829

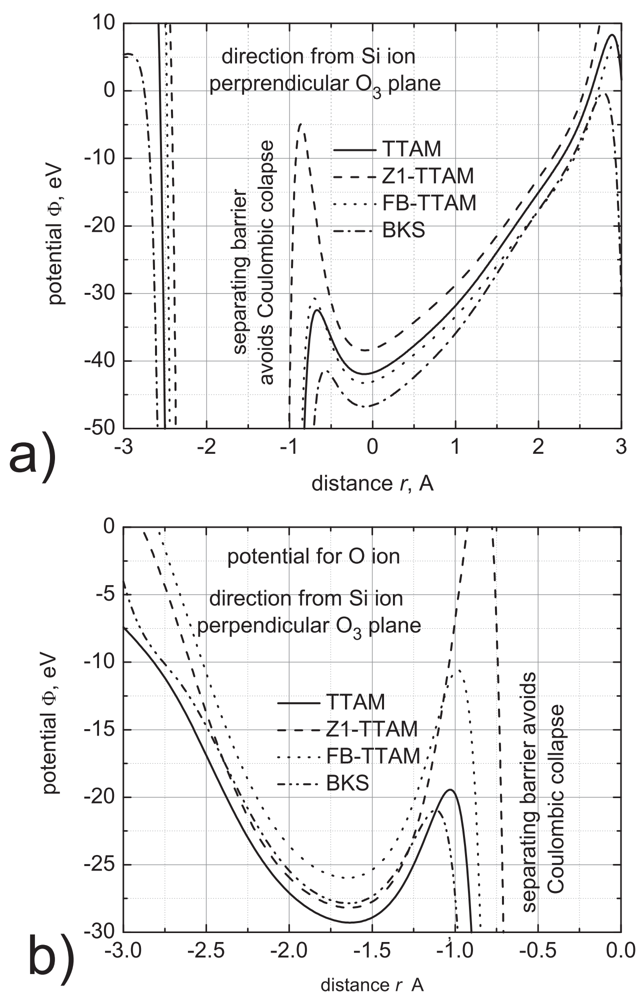

Fig. 4. The potential acting on the Si (a) and O (b) ion from the rest of the crystal in the same direction as in the McPherson Model using various forms of TTAM/BKS pair-wise interatomic potentials.

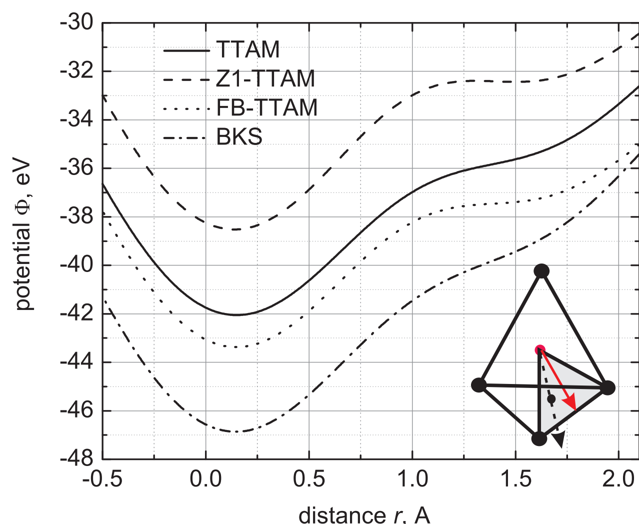

Fig. 5. The potential acting on the Si ion from the rest of the crystal as a function of the ion displacement in the direction from its EP towards the middle of the O-O segment. Inset represents the direction from the center of the SiO_4 tetrahedron towards the secondary minimum: black arrow corresponds to the original McPherson model, red arrow – to the present model.

Fig. 4a shows the potential acting on the Si ion constructed using various types of TTAM/BKS potentials [17-20] as a function of Si ion displacement in the direction from the center of SiO_2 tetrahedron perpendicular to the O_3 plane (the same as in Fig. 1). In this direction these potentials do not feature any ledges, saddle points, etc., as a consequence of the strong effect of the surrounding network (especially of 4 nearest Si neighbors) on the potential profile. All the curves plotted in Fig.4a demonstrate a singularity at $r \sim 1.7$ Å related to the presence of the O ion. Note that potentials are constructed in a way precluding the Coulombic collapse due to relatively high separating barriers in the range of -1…0 Å.

The potential for the O ion reveals an energy minimum at the distance corresponding to the O equilibrium position (see Fig. 4b). A rather high barrier between the EP of oxygen ion and the singularity related to the presence of the silicon precludes the Coulombic collapse (as it was in the case of the potential acting on the Si ion).

We examined other directions and have found a second saddle point in the direction connecting the equilibrium position of the Si ion and the middle of the O-O segment (see Fig. 5, inset) for all types of pair-wise potentials. Fig. 5 demonstrates that in all cases a ledge is situated in the same direction at the same distance of ~ 1.2 Å from Si EP. Fig. 6 represents the 3D potential surface plotted in the plane of the EP of the "selected" Si and two O ions (plane is marked by the gray background in the inset of Fig. 6). This potential profile was calculated using the initial version of the TTAM. In Fig. 6 the Si ion is represented by the blue ball while O ions by black balls. One can see the valley between the two singularities (highlighted by red color) related to the presence of O ions is separated from them by a relatively high barrier precluding the Coulombic collapse. In spite of the fact that the primary

minimum and the saddle point have different energetic positions the difference between them (or the separating barrier in the case of a pronounced secondary minima as it was achieved with Z1 and FB versions of TTAM) are roughly the same, i.e. ~ 6 eV for all forms of TTAM/BKS potentials.

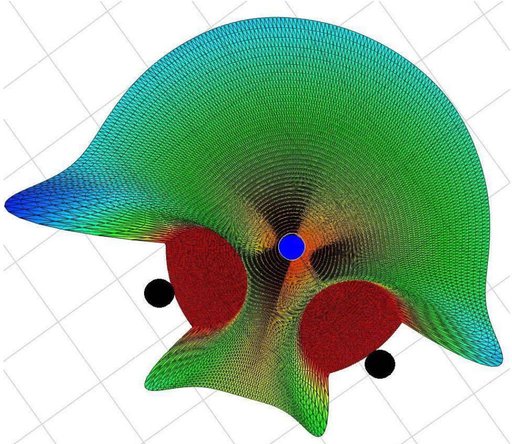

Fig. 6. 3D potential surface plotted in the plane through EP of Si (represented by the blue ball) and 2 O ions (black balls). The potential was calculated using the classical version of TTAM for interatomic interactions.

In the original McPherson model an effective dipole moment p_{eff} = 7…13 eÅ has been reported [4] and thus the interaction of the dipole moment with the electric field provides a contribution to the potential energy of about one eV. However, the high barrier obtained with the Extended McPherson model suggests that the *interaction of the external electric field with the dipole moment is not sufficient for bond-breakage and the contribution of other factors such as captured hole and energy delivered by carriers is needed*. Since several profiles obtained with different forms of TTAM/BKS have the same shape further only the potential based on the initial version of TTAM [17,19] will be used.

V. Effect of Hole Capture and Electric Field

As mentioned above, a high activation energy for the transition of the Si ion between the primary and the secondary minima suggests that the interaction of the dipole moment with the electric field only can not provide a reasonable bond-breakage probability and thus the contribution of another component is essential. One may distinguish 2 various types of these contributions: bond weakening and the energy delivered by particles. Weakening of a bond may be related to hole capture, deviations in Si-O-Si and O-Si-O bond angles [4,21,22], interface mechanical stress [23], structural and topological disorder (see e.g. [24]). The second type assumes an excitation of the bond by the energy deposited by particles, i.e. hot carriers [1,2] and mobile hydrogen [3]. Following McPherson, we examine here the effect of hole capture on the Si-O energetics and consider the effect of the electric field on the rupture of a bond weakened by hole capture.

We assume here that the captured hole is situated in the middle between Si and O ions and thus the contribution of this

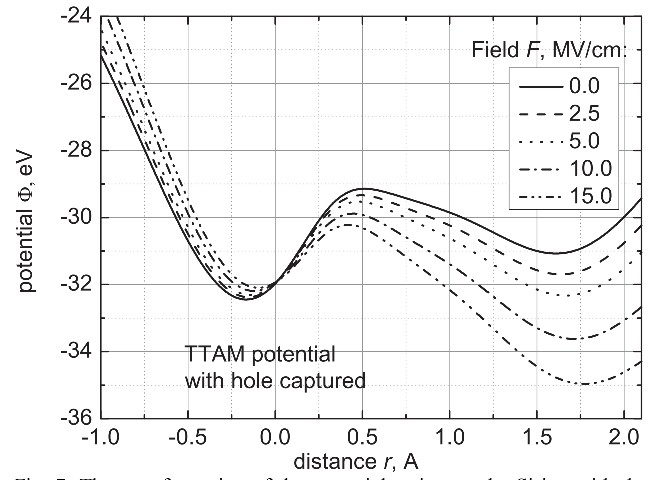

Fig. 7. The transformation of the potential acting on the Si ion with the applied electric field F. The bond is weakened by hole capture.

hole to the potential acting on the Si ion is just the Coulomb potential formed by the positive charge +|e|, i.e.

$$\Phi_{hole} = \frac{+|e| \cdot Q_{Si}}{8\pi\varepsilon_I \varepsilon_0 |\vec{r}_{Si} - \vec{r}_O|}, \tag{10}$$

where ε_I = 3.9 is the insulator permittivity, ε_0 the electric constant and $|\boldsymbol{r}_{Si} - 1/2\cdot(\boldsymbol{r}_{Si} - \boldsymbol{r}_O)| = 1/2\cdot|\boldsymbol{r}_{Si} - \boldsymbol{r}_O|$ is the distance form the hole to the Si ion at the position $\boldsymbol{r}_{Si}$ ($\boldsymbol{r}_O$ is the O ion position).

The net dipole moment of the crystal in equilibrium (i.e. the Si ion at its EP in the center of the SiO_4 tetrahedron) is zero but it develops as silicon is displaced. Following McPherson we write the contribution due to the interaction of the dipole moment with the applied electric field $\boldsymbol{F}$ as:

$$\Phi_{dip}(\vec{r}) = -\vec{p} \cdot \vec{F} = -2|e|\left[\sum_{i=1}^{4} f_i^*(\vec{r} - \vec{r}_i)\right]\left(\frac{2+\varepsilon_I}{3}\right)\vec{F}, \tag{11}$$

where the summation is undertaken over 4 nearest oxygen ions situated in the positions $\boldsymbol{r}_i$; $\boldsymbol{r}$ denotes the radius-vector of the silicon ion. The contribution of each Si-O bond to the dipole moment enters with its polarity, because Si ion bears a charge of +4|e| f_i^* and the O ions -2|e| f_i^*. Note that with the Si ion being at its EP the configuration becomes symmetric, thus f_i^* = f_o^*, $\boldsymbol{r} = 1/4\sum\boldsymbol{r}_i$ and the net moment $\boldsymbol{p}$ is equal to zero as it should be.

To derive the dependency of the bond polarity vs. Si ion displacement let us consider the TTAM pair-wise potential (9) where the first term corresponds to the Coulomb interaction, the second is the repulsive short-range term precluding collapse of the atoms and the third term reflects the covalent component of the bond. Therefore, one may conclude that the bound ionicity is to be found as:

$$f_i^*(r) = \frac{kQ_{Si}Q_O / r}{kQ_{Si}Q_O / r + \gamma_{SiO} / r^6} = \frac{kQ_{Si}Q_O}{kQ_{Si}Q_O + \gamma_{SiO} / r^5}. \tag{12}$$

The profile of the potential acting on the Si ion for the bond weakened by hole capture calculated for various fields F is shown in Fig. 7. One can see that the degeneracy of the primary and the secondary minima occurs at $F_{cr} \sim 5$ MV/cm. This value is lower than that reported in the original McPherson Model, which is 15 MV/cm [4]. Our F_{cr} seems to be more reasonable, especially considering the fact that the dielectric force of the SiO_2 is only 10 MV/cm [25] and under the field of $F \sim 15$ MV/cm SiO_2 film should be already damaged.

VI. Quantization Effects

The transition of the Si ion from the 4-fold coordination to the 3-fold position is treated in this work as bond rupture followed by formation of a Si-Si bridge. This process is treated quantum-mechanically with attraction of the Wentzel–Kramers–Brillouin (WKB) quasi-classical approximation. The bond-breakage is considered as a superposition of two mechanisms: tunneling of the Si ion between the primary and the secondary minima and its thermal excitation over the barrier.

For the calculation of the system of energy levels in the quantum well formed of the primary minimum we employ the Bohr-Sommerfeld quantization:

$$\int_{x_1}^{x_2} \sqrt{2m_{Si}\left(E_n - V(x)\right)dx} = (n+1/2)\pi\hbar\,, \tag{13}$$

with m_{Si} = 28.0855 (in atomic units), $V(x)$ and E_n are the energy profile and the n-th level position, respectively; x_1 and x_2 – are the turning points limiting the classical motion of the Si ion (Fig. 8, inset). The time between two collisions with the potential profile, i.e. allez-retour time is calculated as [26]:

$$\tau_{a-r,n} = 2\sqrt{\frac{m_{Si}}{2}} \int_{x_1}^{x_2} \frac{dx}{\sqrt{E_n - V(x)}} \tag{14}$$

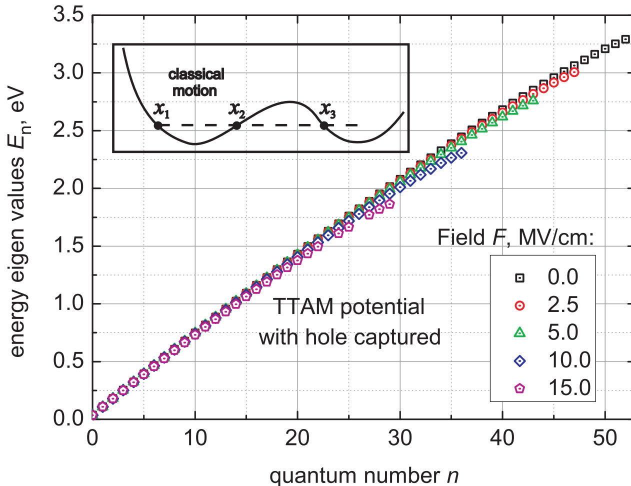

Fig. 8. The ladder of eigen states of the Si ion in the quantum well of the primary minimum calculated for different electric fields F. The inset represents classically allowed and prohibited areas of the Si ion motion.

The occupancy of each level is treated with Boltzmann's distribution, i.e.:

$$f_n = \frac{\exp\left(-E_n / k_B T\right)}{\sum_n \exp\left(-E_n / k_B T\right)}\,, \tag{15}$$

where k_B is Boltzmann's constant and T the absolute temperature. The denominator of (13) represents the statistical sum warranting the probability normalization.

The Si atom on the n-th level undertakes $1/\tau_{a\text{-}r,n}$ attempts per second to tunnel through the barrier (only if the corresponding level has a higher position than the secondary minimum) with the probability:

$$T_n = \exp\left(-\frac{2}{\hbar}\int_{x_2}^{x_3} \sqrt{2m_{Si}\left[V(x) - E_n\right]dx}\right), \tag{16}$$

x_2 and x_3 represent the points restricting the classically prohibited area of Si motion corresponding to the energy E_n (see Fig. 8, inset), i.e. could be found as solutions of the equation $E_n = V(x)$. Summarizing expressions (13-15) one finds the tunneling rate:

$$P_n = \frac{f_n T_n}{\tau_{a-r,n}}\,. \tag{17}$$

VII. Bond-Breakage Rate

The eigenvalues for different values of electric field F are plotted in Fig. 8. With an increase of the field the quantum well becomes shallower and the total number of levels is reduced. Fig. 9 shows the tunneling rate vs. n calculated for various values of F. For low fields (F = 2.5 MV/cm) the offset of Si tunneling is pronounced, because tunneling (without thermal activation) occurs only from energies higher than the bottom of the 2nd minimum. Note, that there is a trade-off between two tendencies: a rapid increase of the tunnel probability T_n with the energy E_n and also rapid decrease of the occupancy f_n vs. E_n accompanied by a weak reduction of the of $1/\tau_{a\text{-}r,n}$. However, f_n aggravates much faster than T_n grows and thus the main contribution to the total bond-breakage rate is provided by a few of the lowest levels.

The dependency of the cumulative bond-breakage rate on the field F for a bond distorted by hole capture is plotted in Fig.10. The change of the slope at ~ 5 MV/cm corresponds to the degeneracy of the prime and the secondary minima resulting in involving all levels into tunneling process.

The thermionic excitation of the Si ion over the barrier E_a is characterized by the rate $P_{th}(E_a) \approx \nu \cdot T_{th}(E_a)$, where $\nu \sim 10^{12} \ldots 10^{13}\ s^{-1}$ is the attempt frequency and $T_{th} = \exp(-E_a/k_B T)$ is the corresponding probability. The dependence of the P_{th} vs. external field F is plotted in the inset of Fig. 10 (we used $\nu = 10^{13}\ s^{-1}$). It is shown, that – contrary to the McPherson model –

the contribution of the thermionic mechanism is by several orders of magnitude weaker than tunneling of the Si ion. This is due to the higher activation energies achieved in the extended model compared to those typical for McPherson model.

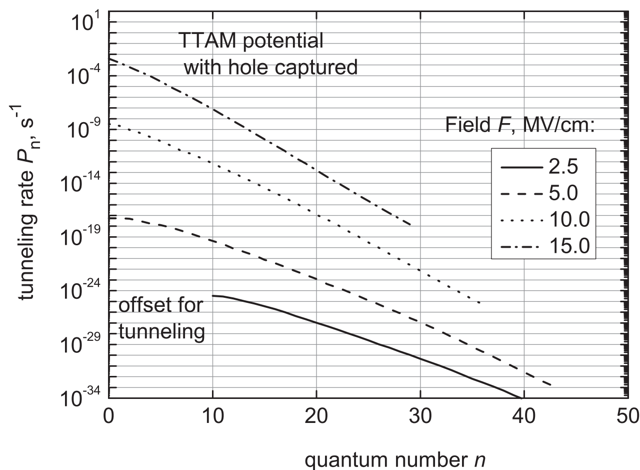

Fig. 9. Tunneling rate as a function of quantum number calculated for different fields *F*.

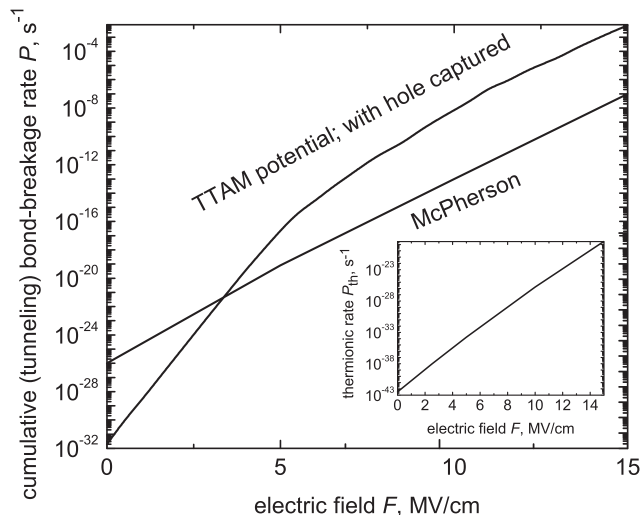

Fig. 10. Bond-breakage rate vs. *F* for the TTAM-based potential with CH compared to those obtained within McPherson model [5].

For comparison, in Fig. 10 we plotted also the rate achieved with the McPherson model (total transmission probability multiplied by attempt rate $\nu \sim 10^{13}$ s^{-1}) for a "virgin" bond [5]. Note, that the difference is 3-4 orders of magnitude for fundamentally distinct scenarios (with/without hole capture) suggests that the *contribution of the whole lattice substantially changes the Si-O bond energetics and drastically reduces the breakage probability*. Therefore, one may conclude that the surrounding network (especially 4 closest Si ions from the neighboring tetrahedrons) stabilizes the Si-O bond and the interaction of the dipole moment with the electric field *only* is not sufficient for providing a considerable bond-breakage rate.

These considerations suggest that a bond weakening by – i.e. captured hole, bond angle variations, build-in of strain, mobile hydrogen (and its species) – is an essential condition for the Si-O bond rupture. Another possible factor is the acceleration of Si ion transmission by the energy delivered by other particles, *hot carriers and/or hydrogen species*, because then the Si ion is excited to a higher level from where it can easily tunnel to the secondary minimum thereby producing a defect.

VIII. Conclusion

In this work, the McPherson model has been extended in a way to capture the effect of the whole surrounding network on the Si-O bond energetics. Within this extended model, Si-Si and O-O interactions were also included which allows us the construction of the potential profile acting on both Si and O ions. Following McPherson, we considered the silicon-excess defect formation (Si-Si bridge), however the developed approach is also suitable for description of the oxygen-excess corresponding to the Si-O-O-Si configuration.

As an initial step we tried to employ the original version of the McPherson model with the Mie-Grüeneisen interatomic pair-wise potential. It was shown that the constants used in the McPherson model are not suitable under consideration of the whole crystal, since the Mie-Grüneisen potential with such parameters can not reproduce the cohesion energy of α-SiO_2 and the potential acting on the O ion reveals an energy maximum (instead of a minimum) at its equilibrium position. In principle, one may find the constants in the Mie-Grüneisen potential by calibration to the results obtained using well-known empirical potentials, namely, TTAM and BKS. But instead of that the way presuming the direct usage of these potentials has been chosen.

We examined various forms of TTAM/BKS potentials and found no ledge in the direction predicted in the McPherson model. Instead, the saddle point was found to occur in the direction connecting the center of the SiO_4 tetrahedron and the middle of the O-O segment for all versions of TTAM/BKS potentials. The effect of the surrounding network does not only shift the position of the secondary minimum but enlarges the activation energy for the transition of the Si ion between the primary and the secondary minima to ~ 6 eV (vs. ~ 2.3 eV reported in the McPherson model). Such a high barrier indicates the fact that the surrounding lattice stabilizes the Si-O bond.

The bond-breakage process has been treated as a transition of the Si ion from the 4-fold coordinated position in the center of the SiO_4 tetrahedron to the 3-fold coordination followed by formation of the Si-Si bridge. This transition is a result of a superposition of two mechanisms: tunneling of the Si ion between the primary and the secondary minima and its thermal excitation over the barrier. Contrary to the McPherson model, it was shown that the main contribution is provided by tunneling (which is by several orders of magnitude higher than thermal excitation). This is due to the fact that in our model

we deal with higher and narrower barriers which are more suitable for tunneling. Another consequence of the presence of the whole lattice is a more realistic value of the electric field (~5 MV/cm) corresponding to the degeneracy between the primary and the secondary minima.

It was revealed that the bond-breakage rates obtained with the McPherson model for a "virgin" bond and that calculated under the consideration of the whole lattice differ by 3-4 orders of magnitude for fundamentally diverse scenarios. Such a behavior suggests that bond rupture purely by means of the electric field is practically impossible. Introduction of a severe bond weakening warrants a reasonable breakage rates demonstrating that only the superposition of field and other factors can lead to defect creation. Among these are a bond distortion and/or its excitation by the energy deposited by particles. The first contribution may be related to hole capture, bond angle (both Si-O-Si and O-Si-O) variations, build-up of stress, structural and topological disorder while the second type presumes the interaction with hot carriers and/or mobile hydrogen and its species.

[1] M. Alam, J. Bude, A, Ghetti, in Proc. of the 38th Annual International Reliability Physics Symposium - IRPS, pp. 21-26 (2000).

[2] S. Mahapatra, D. Saha, D. Varghese, P.B. Kumar, IEEE Trans. Electron Dev., ED-53, No. 7, pp. 1583-1592 (2006).

[3] D.J. DiMaria, J. Appl. Phys., v. 87, No. 12, pp. 8707-8715 (2000).

[4] J.W. McPherson, J. Appl. Phys., v. 99, No. 8, pap. No. 083501, 13 pages (2006).

[5] J.W. McPherson, in Proc. of the 45th Annual International Reliability Physics Symposium - IRPS, pp. 209-215 (2007).

[6] M.Z. Dai, S.I. Kim, A. Yap, Sh. Liu, A. Cheng, L. Yi, Microel. Reliab, v. 48, No. 4, pp. 505-507 (2008);

[7] T.-Ch. Yang, C. Saraswat, IEEE Trans. Electron Dev., ED-47, No. 4, pp. 746-755 (2000);

[8] G. Bersuker, A. Korkin, L. Fonseca, A. Safonov, A. Bagatur'yants, H.R. Ruff, Microel. Engin., v. 69, No. 2-4, pp. 118-129 (2003).

[9] M. Kimura, H. Koyama, Journ. Appl. Phys., v. 85, No. 11, pp. 7671-7681 (1999).

[10] J.W. McPherson, Journ. Appl. Phys., v. 95, No. 12, pp. 8101-8109 (2004).

[11] U. Essmann, L. Perera, L. Berkowitz, T. Darden, H. Lee, L.G. Pedersen, J. Chem. Phys., v. 103, No. 19, pp. 8577-8593 (1995).

[12] A. Grzybowski, E. Gwóźdź, A. Bródka, Phys. Rev. B, v. 61, No. 10, pp. 6706-6712 (2000).

[13] A. Tandia, G. Sarrabayrouse, A. Martinez, Thin Solid Films, v. 296, No. 1-2, pp. 122-125 (1997).

[14] F. Jollet, C. Noguera, Phys. Stat. Sol. (b), v. 179, No. 2, pp. 473-478 (1993).

[15] J.D. Gale, J. Chem. Soc., Faraday Trans., v. 93, No. 4, pp. 629-637 (1997).

[16] VASP, the Guide, http://cms.mpi.univie.ac.at/vasp/vasp/vasp.html.

[17] S. Tsuneyuki, M. Tsukada, H. Aoki, Y. Matsui, Phys. Rev. Lett., v. 61, No. 7, pp. 869-872 (1998).

[18] B.W.H. van Beest, G.J. Kramer, R.A. van Santen, Phys. Rev. Lett. v. 64, No. 16, pp. 1955-1958 (1998).

[19] A.R. Al-Derzi, M.G. Gory, K. Runge, S.B. Trickey, J. Phys. Chem. A, v. 108, No. 52, pp. 11679-11683 (2004).

[20] W. Zhu, K. Runge, S.B. Trickey, J. Comp.-Aid. Mater. Design, v. 13, No. 1-3, pp. 75-84 (2006).

[21] S. Munetoh, T. Motooka, K. Moriguchi, A. Shintani, Comput. Material Sci., v 39, No. 2, pp. 334-339 (2007).

[22] A. Carré, J. Horbach, S. Isoas, W. Kob, Lett. Journ. Expl. Frontiers Phys., v. 82, No. 1, pap. No: 17001 (2008).

[23] T.-Ch. Yang, C. Saraswat, IEEE Trans. Electron Dev., ED-47, No. 4, pp. 746-755 (2000).